Optica Applicata, Vol. XLVIII, No. 4, 2018
10.5277/oa180402

Two-point resolution with spherical aberration quadratic amplitude filters

Naresh Kumar Reddy ANDRA[1, 3, 4*], Svetlana Nikolaevna KHONINA[1, 2]

[1]Samara National Research University, Moskovskoye Shosse, 34, 443086, Samara, Russia

[2]Image Processing Systems Institute – Branch of the Federal Scientific Research Centre "Crystallography and Photonics" of Russian Academy of Sciences, 443001, Samara, Russia

[3]School of Engineering, Anurag Group of Institutions, Venkatapur, Ghatekesar, Medchal District, Hyderabad, 500088, Telangana, India

[4]Nir Davidson and Asher A. Friesem Lab, Department of Physics of Complex Systems, Weizmann Institute of Science, 7610001 Rehovot, Israel

[*]Corresponding author: naarereddy@gmail.com, naarereddy@ssau.ru

The study deals with the effects of spherical aberration on the Airy distribution of two overlapping point images of equal- or unequal-intensities separated by the distances less than the Rayleigh angular limit of resolution investigated. Aberration considered in this work is the primary spherical aberration. By employing the quadratic amplitude apodization across the aperture, the high resolution is achieved in the form of resolving the two-point images, which is higher than that of the unapodized ones. In this investigation, the apodization mask applied to the aperture and the corresponding intensity distributions of two-point images have been studied numerically.

Keywords: coherence, apodization, superresolution.

1. Introduction

An image-forming system in the presence of the optical aberrations has become very important in many potential applications. The manufacturing of the optical imaging instrument and the environment in which it operates can play a vital role in the reduction of the aberrations. Aberration leads to defects in the imaging wave front of the optical system. Certainly the effects of the aberrations on the performance of the optical system can be controlled by the apodization technique. The apodization is achieved by altering the shape or size of the optical elements integrated in the optical system. The process of the amplitude apodization deliberately modifies the light transmittance of the optical system. This technique significantly changes the amplitude impulse response and the imaging characteristics of the optical system under any degree of the coherence of the illumination. For aberrated optical systems under different consider-

ations, by employing the apodization, its resolving power is significantly improved. There are a number of systematic studies reported in the recent past in which the resolution of the two point objects or the point object was investigated under the influence of different types of optical aberrations and the apodization. In these studies, the optical system performance was characterized by the amplitude or phase mask pupils. Usually the pupil function with the apodization was very effective in the elimination of the sidelobes and the sharpening of the central spot in the field distribution and also useful to resolve the two overlapping point sources separated by the distance which is more or less than the Rayleigh's angular limit of resolution. Asakura *et al.* [1, 2] investigated the resolution of two unequally bright point sources under the incoherent light illumination by means of the Sparrow criterion. Mills and Thompson [3] made a systematic study on the effect of aberrations and apodization on the amplitude impulse response of the coherent optical systems. Hazra *et al.* [4–6] introduced methods of compensating the aberrations and the atmospheric turbulence effect on the performance of the optical system. Biswas and Boivin [7, 8] investigated the influence of the spherical and astigmatism aberrations on the efficiency of the optimizing apodized optical systems. Sagar *et al*. [9] studied the effect of the defocusing and the shaded aperture on the Sparrow limits of the two bright points with widely varying intensities and continued their work [10] on the defocusing aberration influence on the two-line resolution of the coherent optical system with Hanning amplitude filters. Ratnam *et al*. [11] investigated the maxima and minima of the diffracted point image with the MACA and CMACA aperture systems. More studies in this trend [12–24] were mainly focused on the altering of the aperture into the suitable form which was employed to modify the transmittance of the optical system in a direction to improve the resolution. All these studies are the motivation for the current investigation.

In the present work, in addition to the amplitude apodization applied to the circular aperture in the form of the amplitude parabolic filters of the superresolving type, we investigated the effect of aberrations on the two equal and unequal intensity point sources separated by the small distances less than that of the limit of resolution. The effects of the degree of the coherence and the intensity ratio of the two-point sources are also analyzed for different amounts of the primary spherical aberration. These studies are very potential in different image forming systems. However, the resolution of the two overlapping point images was primarily considered in the fields of astronomy, confocal microscopy, and spectroscopic observations. In other words: imaging of the far-distant objects where the amplitude shade was applied across the objective lens of the telescope, detection of the closely associated spectral points by employing the shaded plate at the entrance of the spectrometer aperture and resolving the two closely located point structures of the biological specimen with the objective lens of the suitable shade.

2. Theory

Following the scalar-wave diffraction theory, the intensity distribution in the image plane is the Fourier transform of the light distribution across the circular pupil function

in the object plane. The composite image intensity distribution of overlapping point images formed by the apodized optical imaging system is given by [25–27]

$$I(V) = |A(V-B)|^2 + c|A(V+B)|^2 + 2\sqrt{c}\,\gamma(V_0)|A(V-B)||A(V+B)| \tag{1}$$

where $2B = V_0$ is the distance separation between two point sources, c is the intensity ratio of the sources, $\gamma(V_0)$ is the real part of the complex degree of the coherence of illumination, V is the dimensionless diffraction variable, $A(V+B)$ and $A(V-B)$ are the amplitude impulse responses of the optical imaging system corresponding to the two point sources. The two points are located at the distance of $V_0/2$ on either side of the optical axis.

The image amplitude impulse response functions of point images are given by

$$A(V \pm B) = 2\int_0^1 J_0((V \pm B)u)u\,\mathrm{d}u \tag{2}$$

Here J_0 is the Bessel function of first kind and zero order, u is the radial coordinate in the pupil plane, which is also defined as the normalized distance of a general point on the exit pupil of the optical system varying from 0 to 1. In the present work, we employed the quadratic amplitude filter across the exit of the circular pupil function, then Eq. (2) can be written as

$$A(V \pm B) = 2\int_0^1 g(u)J_0((V \pm B)u)u\,\mathrm{d}u \tag{3}$$

Here, $g(u) = u^2$ is the parabolic amplitude apodizer, employed across the circular aperture in the exit pupil plane of the apodized optical system. The amplitude transmittance of the parabolic filter is a function of the dimensionless variable u, thus, the transmittance increases from the center to the periphery of the aperture. It is illustrated in Fig. 1 in more detail. The resultant amplitude impulse response of the parabolic amplitude apodizer across the pupil function is given as follows:

$$A(V \pm B) = 2\int_0^1 u^2 J_0((V \pm B)u)u\,\mathrm{d}u \tag{4}$$

The aberration considered in this study is represented by the spherical wave front $\Phi(u, \theta)$, given by

$$\Phi(u, \theta) = \exp\left(-i\varphi_s \frac{u^4}{4}\right) \tag{5}$$

In optical microscopy [28], the term used by the primary spherical aberration is

$$\Phi(\rho; w_{40}, \alpha) = \exp\left\{ i\pi w_{40} \frac{\left[1 - \sqrt{1 - \rho^2 \sin(\alpha)}\right]^2}{2\sin^4(\alpha/2)} \right\} \tag{6}$$

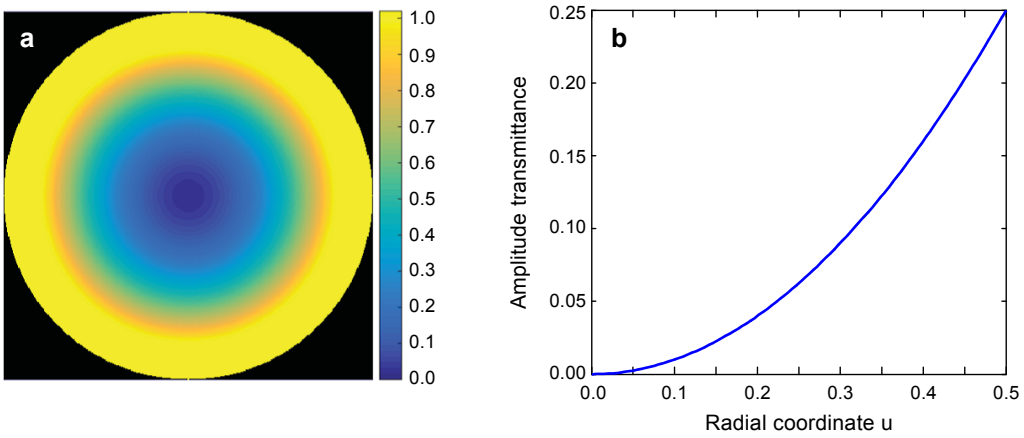

Fig. 1. The amplitude transmittance of the pupil mask: the amplitude distribution across the circular pupil (**a**), and the amplitude transmittance of the pupil varies with the radial coordinate u (**b**).

However, we should note that Eq. (6) is actual for the microscopy-optical systems where NA is very high. In our investigations, we rather regard a paraxial-optical system, so NA is small (for free space $\ll 1$) and we can rewrite the approximations used

$$1 - \sqrt{1 - \rho^2 \sin(\alpha)} \approx 1 - 1 + \frac{1}{2}\rho^2 \sin(\alpha) = \frac{1}{2}\rho^2 \sin(\alpha) \tag{7}$$

After redesignation:

$$u = \rho \quad \text{and} \quad \varphi_s = \pi w_{40} \frac{\sin^2(\alpha)}{2\sin^4(\alpha/2)} \tag{8}$$

we obtained Eq. (5) instead of Eq. (6). Here φ_s is the amount of the primary spherical aberration. The image-plane field distribution arising from the two-point sources is proportional to the Fourier transform of the field distribution across the exit pupil mask of the aberrated optical system. The amplitude transmittance of the apodized optical system with the primary spherical aberration can be written as

$$A(V \pm B) = 2\int_0^1 u^2 \exp\left(-i\varphi_s \frac{u^4}{4}\right) J_0((V \pm B)u)u\,\mathrm{d}u \tag{9}$$

To estimate the possibility of compensating the spherical aberration by amplitude quadratic apodization, we calculate modulation transfer function (MTFs) (Fig. 2). As seen from Fig. 2, the introduction of the quadratic amplitude filter provides higher spatial frequency under the Rayleigh limit, which means that the resolution limit is improved. In the presence of spherical aberration, the filter also provides some improvement.

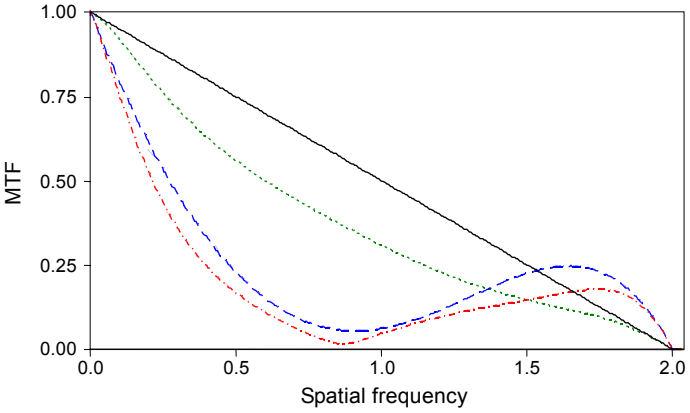

Fig. 2. MTF for conventional system (solid line), aberrated system with $\varphi_s = 2\pi$ (dotted line), apodized system (dashed line), and aberrated and simultaneously apodized system (dash-dot line).

Note that the apodized point spread function (PSF) can provide superresolution due to the growth of the sidelobes. This is not good for the classical imaging system when we use common/usual pictures. However, this can help solve the problem of resolving two points [1–3].

The total image intensity distribution of overlapping two point sources under different considerations and the primary spherical aberration have been obtained by substituting Eq. (9) in the general expression Eq. (1).

3. Results and discussion

The results of investigations on the two-point intensity distributions of the optical system with a superresolving amplitude filter have been studied from Eq. (1). An iterative method of numerical integration has been developed and applied to compute the results in the application of the two-dimensional amplitude mask. The computed intensity distributions with the amplitude shaded circular aperture show that the two point images are well resolved and the resolving power of the apodized optical system is highly improved, better than that of the Airy PSF distributions.

Figure 3**a** gives the irradiance distribution of two point objects with equal intensities, separated by the limits V_0 lower than that of the Rayleigh angular limit (3.832 = $= 1.22\lambda/D_{\text{aperture diameter}}$) for the Airy pupil. When the two point objects are separated by a distance of $V_0 = 3.0$, a dip of intensity in the profile curve is almost equal to zero, *i.e.* two point sources are unresolved. The resolution and the dip on the intensity distributions is found only when the limit V_0 is higher than $V_0 = 3.0$. In the presence of the parabolic amplitude filter, the Airy intensity distribution is modified and it has been shown in Fig. 3**b**. As the distance of the separation V_0 between the two point images increases, the position of the central dip moves toward the low intensity maximum.

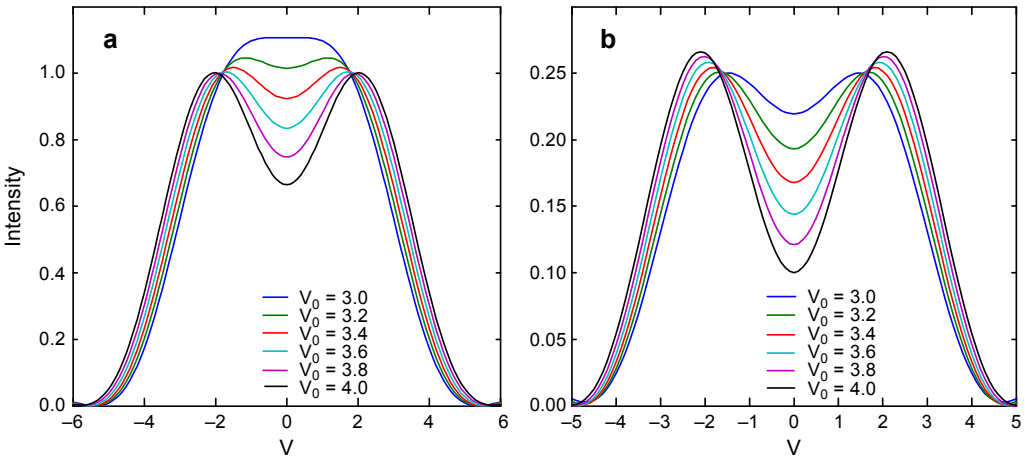

Fig. 3. The image intensity distribution of two equal-irradiance (c = 1) point sources separated by the limits V_0 (3.0 → 4.0) under the incoherent illumination (γ = 0) formed by: the Airy pupil (**a**), and the apodized pupil (**b**).

Hence, the images of closely located two point sources are well resolved. In the case of the V_0 = 3.0, the dip position on the profile curve is clearly visible, *i.e.* by employing the shaded aperture, the resolution of two equal irradiance Gaussian image points is improved and achieves the super-two-point resolution. It is clear in Fig. 3 that for the measurable separation (V_0 = 4.0) of two point images which is bigger than the incoherent Rayleigh limit, the intensity distribution in the Airy case due to the two point sources is tailored into the high resolution component by the apodized pupil.

Figure 4**a** illustrates the image intensity distribution of two point sources with unequal intensities, separated by the distances shorter than that of the Rayleigh angular

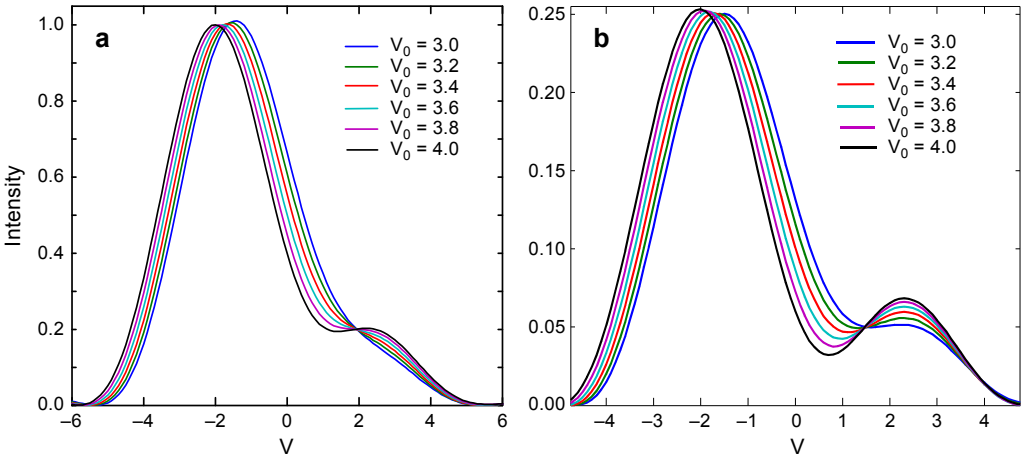

Fig. 4. The irradiance distribution of two unequal-irradiance point sources (c = 0.2) of the optical system under the incoherent light illumination formed by: the Airy pupil (**a**), and the apodized pupil (**b**).

limit through the unapodized pupil. The two images are not resolved, but the resolution is little improved for the higher value of V_0. For the $V_0 = 4$, the dip on the composite intensity profile of the two point sources is clearly visible whereas in the case of the amplitude apodized optical system, the resolution is higher than that of the unapodized one. Figure 4**b** shows that the two point images are resolved, due to the clear presence of the dip on the resultant intensity distribution of the two point objects. It is observed that as the V_0 increases, the position of the dip shifts toward the center of the resultant intensity profile and finally obtains low intensity maximum. This shift in the resultant intensity profile is due to the movement of the principal maxima of the two points away from each other.

3.1. Spherical aberration

The primary spherical aberration has the functional form $\Phi = \exp[-i\varphi_s(u^4/4)]$ which is a radially variant aberration and its fourth power dependence is associated with the radial coordinate u of the aperture. It is due to the deviation of the spherical wave front from its ideal shape. The presence of the primary spherical aberration is the origin of changes in the image-plane optical field distribution, such as a decrease in the Strehl ratio, increase in the first-sidelobe energy, and shift in the position of the first minima. However, the amount of change in the field distribution depends on the value of the spherical aberration. In the presence of the primary spherical aberration, the image intensity distribution of the optical system when the amplitude apodizer is employed is shown in Fig. 5.

Figure 5**a** shows the image intensity distribution of two equal-irradiance point sources separated by the limits lower than the Rayleigh limit under the incoherent illumination ($\gamma = 0$) through an unapodized optical system. For any given value of the spherical aberration ($\varphi_s = 0 \rightarrow 2\pi$), the object points separated by a distance of $V_0 = 3.0$

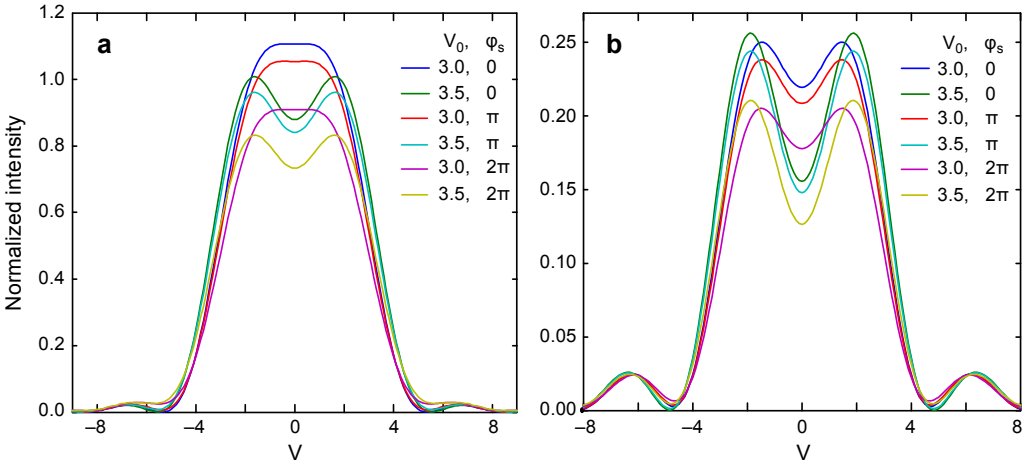

Fig. 5. Spherical aberration φ_s effect on the image intensity distribution of two equal intensity ($c = 1$) point images separated by the distances $V_0 = 3.0$ and 3.5 for the unapodized pupil (**a**), and the apodized pupil (**b**).

are not resolvable, due to the fact that the resultant peak came from overlapping of the central peaks of both point sources, but for $V_0 = 3.5$, the two point images are resolved, *i.e*. the presence of the central dip on the profile curves is clearly visible. However, Fig. 5**b** illustrates the composite image intensity distribution for the two point sources of the apodized optical system. The two point images are resolved perfectly, much better than those of the unapodized ones. As the value of V_0 increases from 3.0 to 3.5, the resolution of the optical system also increases.

By employing the parabolic amplitude filter, the intensity of the central dip on the resultant profile of the two images increases and obtains the low intensity maximum, relatively with that of the Airy case. In the presence of amplitude apodization, the intensity of the central dip on the image intensity distribution of the aberrated optical system is higher than that of the central dip intensity on the resultant image field distribution of the unapodized optical system with the spherical aberration φ_s. For the apodized pupil, there exists a shift in the position of the first minima which has taken place towards the principal maxima of the resultant field distribution.

Figure 6 illustrates that in the presence of the spherical aberration φ_s, as the degree of the coherence γ increases from 0 to 1 in steps of 0.5, the resolution of overlapping point images decreases. For $\gamma = 0$, the two-point images separated by a distance $V_0 = 3.5$ through an apodized optical system are found with the high resolution. Figure 6**a** shows that in the presence of partial spherical aberration ($\varphi_s = \pi$) for $c = 0.2$ and 1, as γ increases, the intensity of the central dip on the intensity distribution decreases and vanishes, whereas for $\varphi_s = 2\pi$ the intensity of the dip decreases with the values of γ but the position of the dip is clearly found in all considerations with finite intensity which is shown in Fig. 6**b**. It emphasizes that in the presence of high spherical aberration ($\varphi_s = 2\pi$), the amplitude in the apodized optical system results in the performance based on resolving

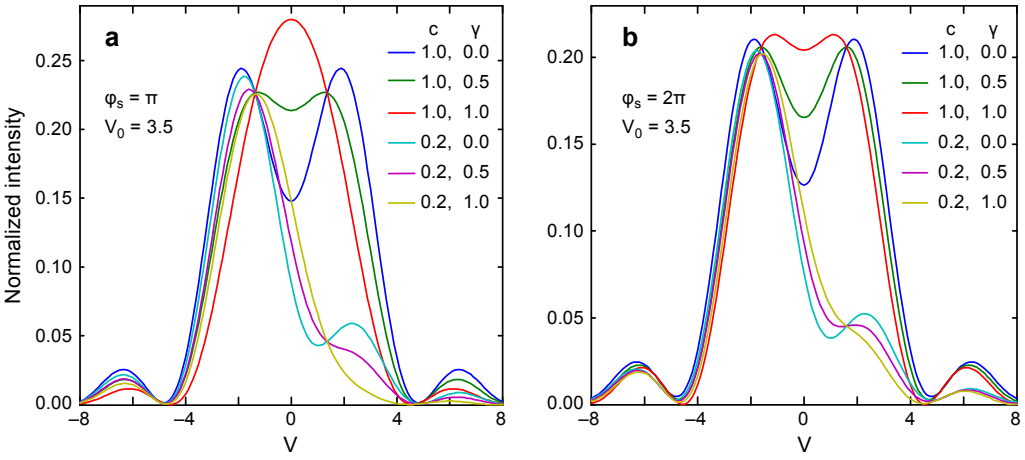

Fig. 6. The image intensity distribution of the two equal ($c = 1$) and unequal ($c = 0.2$) intensity point images separated by the distance $V_0 = 3.5$ under the different degree of the coherence of the illumination γ for the spherical aberration $\varphi_s = \pi$ (**a**), and $\varphi_s = 2\pi$ (**b**).

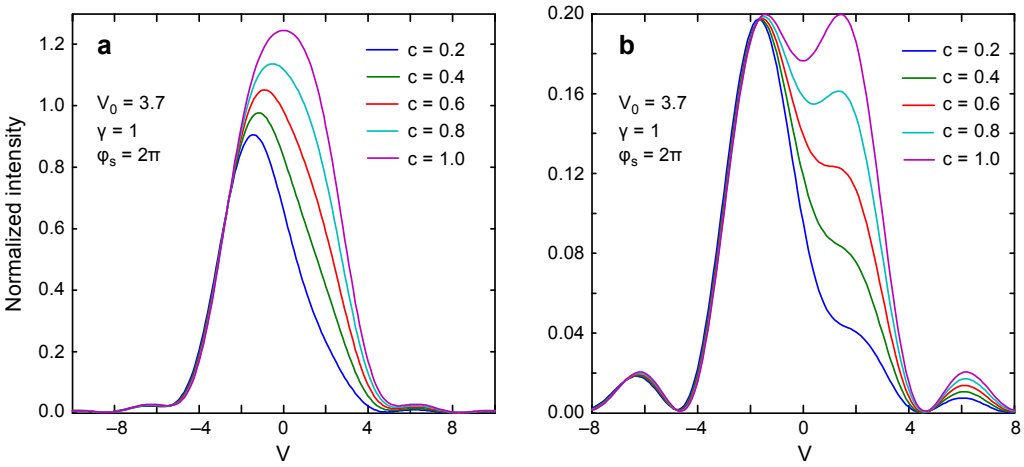

Fig. 7. Spherical aberration made image distribution of the two points with a different intensity ratio c under the coherent illumination ($\gamma = 1$) for the unapodized pupil (**a**), and the apodized pupil (**b**).

the two equal- or unequal-irradiance point sources under any degree of the coherence of illumination.

Figure 7**a** illustrates the image intensity distribution of two point images with different intensity ratios separated by the distance $V_0 = 3.7$ under the coherent light illumination through the unapodized system. In the presence of high spherical aberration $\varphi_s = 2\pi$, the resultant intensity distribution is produced from the closest approach of the diffraction patterns of the two points. In this case, the two points are not resolved from the intensity distribution profile in the image plane. For the aberrated optical system with the parabolic amplitude apodizer, the resultant intensity curves are shown in Fig. 7**b**.

The curves show a distinct dip in the middle of two principal maxima, *i.e.* the dip is clearly noticed with the finite intensity in between the diffraction patterns of the two points. Thus the two point images are distinguished from one another and they are just resolved for higher degrees of intensity ratio. So the apodizer is effective, while the resolution of the apodized intensity distribution of two nearest point images is much better than the unapodized case.

3.2. Resolution of two equal intensity object points under various conditions of coherence

In this section, the effect of the degree of coherence is investigated. In Fig. 8, the value $V_0 = 3.6$, is the distance separation lower than that for the incoherent Rayleigh limit (3.832). In the presence of the aberration-free Airy pupil, the two-point sources are resolved for the values of γ varying from –1 to 0.3, as is clearly presented by the distinct dips in the resultant intensity distribution. As γ increases from 0.3 to 1.0, the dip in the middle of the composite image intensity distribution vanishes. Hence the two points are not resolved, whereas by employing the quadratic amplitude apodization across the

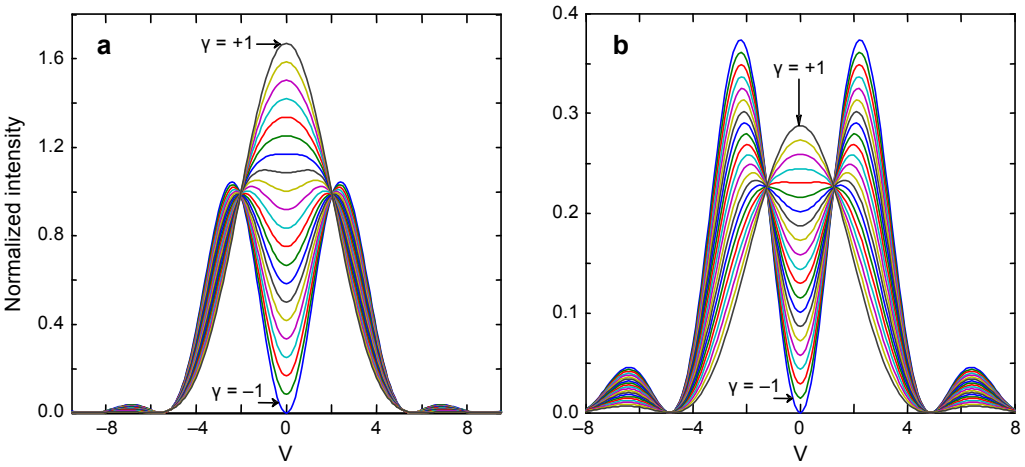

Fig. 8. Distribution of two-equal intensity point sources for various values of γ from –1.0 to +1.0 in steps of 0.1 for $V_0 = 3.6$ for Airy pupil (**a**), and apodized pupil (**b**).

circular aperture, the two principal maxima in the resultant intensity curve move away as the degree of coherence increases from 0 to +0.5.

Figure 8**b** illustrates that as γ is decreasing from 0 to –1, the limit of resolution is reaching the infinite value under the conditions of antiphase coherence. Hence, the two-points in phase opposition are well resolved. In this case, the measured dip intensities are lower, compared to those of the Airy case. It has been found that the two-point resolution under the partially coherent illuminance is excellent, which is manifested by the presence of a distinct dip in the composite intensity distribution of two object points with equal intensities. For high coherence conditions of illuminance, with no

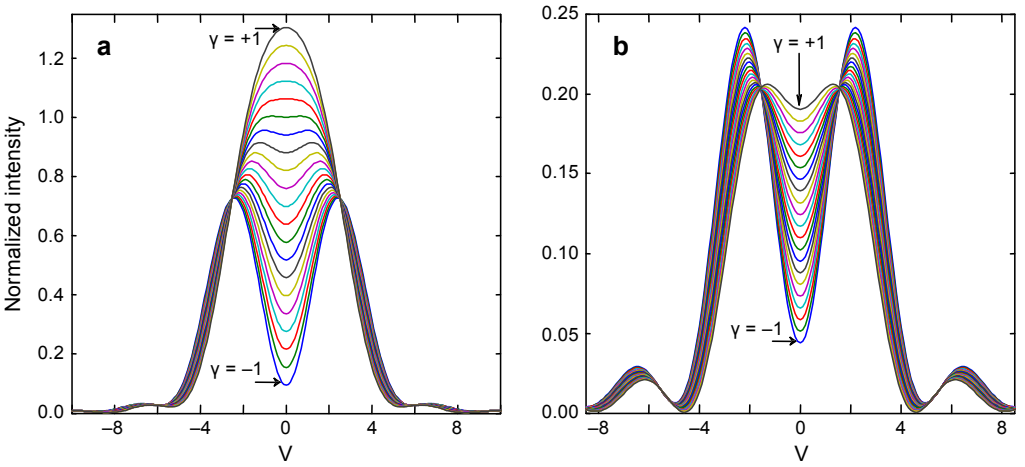

Fig. 9. Composite image intensity distribution for two equal intensity point sources separated by the distance $V_0 = 3.6$ in the presence of high spherical aberration ($\varphi_s = 2\pi$), the degree of coherence γ ranging from –1.0 to +1.0 for Airy pupil (**a**), and apodized pupil (**b**).

indication of a dip in the resultant intensity curve, the points are said to be unresolved. A similar set of curves for $V_0 = 3.6$ in the presence of high spherical aberration, has been shown in Fig. 9. For the aberrated Airy pupil, two-point sources are resolved in the limit of degree of coherence γ varying from –1.0 to +0.3. Here it is observed that the resolution decreases as the degree of coherence increases, as is evidenced by the curves which are essentially becoming flat and the dip in the composite intensity distribution almost vanishes. As γ increases, the diffraction pattern of the individual point objects results in the intensity distribution without any dip.

Another set of curves with the distance separation $V_0 = 3.6$ is displayed in Fig. 9**b**. By employing the spherical aberration ($\varphi_s = 2\pi$) in apodized circular pupils, the two points are resolved for all the coherence conditions. As is proved by the presence of the distinct dips, the two point sources are well resolved for all values of γ. In this case, the resolving power of the apodized optical system is said to be excellent in the anti-phase and in-phase coherence region. As the degree of coherence increases, the principal maxima in the distribution shift are closer to each other which results in the small measured separation. It has been observed that in the presence of high spherical aberration, the apodized system proved to be very effective and accurate in resolving the two point sources for all conditions of illumination.

4. Conclusion

It has been found that the efficiency of the two-point imaging of the aberrated optical systems with the quadratic amplitude apodization filters depends upon the degree of the coherence of light illumination γ. It is concluded that in the presence of the primary spherical aberration, the resolution of the two point sources separated by the distance smaller than the Rayleigh limit under the coherent light illumination (γ =1) has been increased by the proposed apodizer. As it is proved by the clear presence of a dip in the intensity distributions, the point images are well resolved for all the values of the intensity ratio of the sources c. Under the presence of the spherical aberration, as the illumination approaches to the incoherent limit, the principal maxima in the resultant image intensity distribution move away from each other generating a clear separation which is measured with high accuracy. It is emphasized that in this paper the resolution of the two-point imaging of the apodized optical system is considerably improved in comparison to that of the unapodized one. Note that the apodized PSF can provide superresolution due to the growth of the sidelobes. This is not good for the classical imaging system when we use common/usual pictures. However, this can help solve the problem of resolving two points [1–3]. For aberration that is not circularly symmetric, *i.e*. coma, astigmatism, the resulting Airy intensity distribution due to the two -point sources will be analyzed with apodized systems at a focus in the next paper.

Acknowledgements – This work was financially supported by the Ministry of Education and Science of Russian Federation in the framework of the government contract 3.5319.2017/8.9, the Israel Science Foundation (ISF) and the Russian Foundation for Basic Research (Grants 16-29-11698, 16-07-00825).

References

[1] Asakura T., *Resolution of two unequally bright points with partially coherent light*, Nouvelle Revue d'Optique **5**(3), 1974, pp. 169–177.

[2] Asakura T., Ueno T., *Apodization for increasing two-point resolution by the sparrow criterion under the partially coherent illumination*, Nouvelle Revue d'Optique **5**(6), 1974, pp. 349–359.

[3] Mills J.P., Thompson B.J., *Effect of aberrations and apodization on the performance of the coherent optical systems. I. The amplitude impulse response*, Journal of the Optical Society of America A 3(5), 1986, pp. 694–703.

[4] Hazra L.N., Purkait P.K., De M., *Apodization of aberrated pupils*, Canadian Journal of Physics 57(9), 1979, pp. 1340–1346.

[5] De M., Hazra L.N., *Real-time image restoration through walsh filtering*, Optica Acta: International Journal of Optics 24(3), 1977, pp. 211–220.

[6] De M., Hazra L.N., *Walsh functions in problems of optical imagery*, Optica Acta: International Journal of Optics 24(3), 1977, pp. 221–234.

[7] Biswas S.C., Boivin A., *Influence of spherical aberration on the performance of optimum apodizers*, Optica Acta: International Journal of Optics 23(7), 1976, pp. 569–588.

[8] Biswas S.C., Boivin A., *Influence of primary astigmatism on the performance of optimum apodizers*, Journal of Optics (Paris) **4**, 1975, pp. 1–11.

[9] Keshavulu R. Sayanna, Karuna Sagar D., Goud S.L., *Effects of defocusing on the Sparrow limits for apodized optical systems*, Optics Communications 217(1–6), 2003, pp. 59–67.

[10] Karuna Sagar D., Biskshamaiah G., Keshavulu Goud M., Goud S.L., *Defect of focus in two-line resolution with Hanning amplitude filters*, Journal of Modern Optics 53(14), 2006, pp. 2011–2019.

[11] Ratnam C., Lakshmana Rao V., Goud S.L., *Comparison of PSF maxima and minima of multiple annuli coded aperture (MACA) and complementary multiple annuli coded aperture (CMACA) systems*, Journal of Physics D: Applied Physics 39(19), 2006, pp. 4148–4152.

[12] Nayyar V.P., Verma N.K., *Two-point resolution of Gaussian aperture operating in partially coherent light using various resolution criteria*, Applied Optics 17(14), 1978, pp. 2176–2180.

[13] Kumar Reddy A.N., Karuna Sagar D., *Two-point resolution of asymmetrically apodised optical systems*, Óptica Pura y Aplicada 46(3), 2013, pp. 215–222.

[14] McKechnie T.S., *The effect of condenser obstruction on the two-point resolution of microscope*, Optica Acta: International Journal of Optics 19(9), 1972, pp. 729–737.

[15] Sheppard C.J.R., Hegedus Z.S., *Axial behavior pupil-plane filters*, Journal of the Optical Society of America A 5(5), 1988, pp. 643–647.

[16] Ojeda-Castañeda J., Berriel-Valdos L.R., Montes E., *Spatial filter for increasing the depth of focus*, Optics Letters 10(11), 1985, pp. 520–522.

[17] Magiera L., Pluta M., *Image quality criteria of the apodized optical systems with spherical aberrations with one- and two-point imaging*, Optica Applicata **11**(2), 1981, pp. 231–241.

[18] Sirohi R.S., *Limit of resolution of diffraction limited circular aperture for line objects*, Optik **29**, 1969, pp. 437–439.

[19] Falconi O., *Limits to which double lines, double stars, and disks can be resolved and measured*, Journal of the Optical Society of America 57(8), 1967, pp. 987–993.

[20] Gupta S.V., Sen D., *Diffrimoscopic image formation under partially coherent illumination (slits and opaque strips)*, Optica Acta: International Journal of Optics 18(10), 1971, pp. 779–792.

[21] Grimes D.N., Thompson B.J., *Two-point resolution with partially coherent light*, Journal of the Optical Society of America 57(11), 1967, pp. 1330–1334.

[22] Hopkins H.H., Zalar B., *Aberration tolerances based on the line spread function*, Journal of Modern Optics 34(3), 1987, pp. 371–406.

[23] Khonina S.N., Ustinov A.V., Pelevina E.A., *Analysis of wave aberration influence on reducing focal spot size in a high-aperture focusing system*, Journal of Optics 13(9), 2011, article ID 095702.

[24] KLEBANOV I.M., KARSAKOV A.V., KHONINA S.N., DAVYDOV A.N., POLYAKOV K.A., *Wave front aberration compensation of spacecraft telescopes with telescope temperature field adjustment*, Computer Optics 41(1), 2017, pp. 30–36.
[25] HOPKINS H.H., BARHAM P.M., *The influence of the condenser on microscopic resolution*, Proceedings of the Physical Society. Section B **63**(10), 1950, pp. 737–744.
[26] BORN M., WOLF E., *Principles of Optics: Electromagnetic Theory of Propagation, Interference and Diffraction of Light*, 7th Ed., Cambridge University Press, Cambridge, 1999, p. 986.
[27] GOODMAN J., *Introduction to Fourier Optics*, Roberts and Company Publishers, 2005.
[28] ESCOBAR I., SÁNCHEZ-ORTIGA E., SAAVEDRA G., MARTÍNEZ-CORRAL M., *New analytical tools for evaluation of spherical aberration in optical microscopy*, [In] *Optical Fluorescence Microscopy*, [Ed.] A. Diaspro, Springer, Heidelberg, 2011.

Received October 27, 2017
in revised form January 1, 2018